Histol Histopathol (2017) 32: 1207-1221

http://www.hh.um.es

Histology and Histopathology

From Cell Biology to Tissue Engineering

Sialic acid expression in human fetal skeletal muscle during limb early myogenesis

Mirca Marini[1], Erica Sarchielli[1], Giorgia Donata Zappoli Thyrion[2], Stefano Ambrosini[1] and Eleonora Sgambati[3]

[1]Department of Experimental and Clinical Medicine, Section of Anatomy and Histology, Careggi Hospital, [2]Department of Surgery and Translational Medicine, Careggi Hospital, University of Florence, Florence and [3]Department of Biosciences and Territory, University of Molise, Pesche (Isernia), Italy

Summary. Investigations on animal models demonstrated that changes of sialic acid (SA) expression, particularly the polymeric form, in the skeletal muscle during embryonic and post-natal development seem to be related to muscle differentiation and functionality onset. The aim of this study was to evaluate the monomeric and polymeric SA expression in human skeletal muscle during early stages of fetal development, when important morphofunctional events occur. Specimens of fetal skeletal muscle from limb, between 9 and 12 weeks of gestation (wg), were obtained from 19 pregnant women. To investigate some morphofunctional features occurring during this development period, haematoxylin-eosin staining, tunel assay and immunohistochemistry for connexin-43 (Cx43) and parvalbumin were performed. SA expression and characterization was evaluated using lectin histochemistry (MAA, SNA, PNA, SBA, DBA), associated with enzymatic and chemical treatments. Polysialic acid (PSA) expression was also evaluated using immunohistochemistry. The results showed apoptotic myotubes between 9 and 10.5 wg, disappearing from 11 wg; Cx43 was more abundant in myotubes/myoblasts between 9 and 9.5 wg, decreasing and/or disappearing from 10 wg and parvalbumin was present in myotubes between 10 and 10.5 wg. PSA was revealed in myotubes/myoblasts from 9 to 10.5 wg; from 11 wg it was reduced or disappeared. Monomeric SA appeared in myotubes/myoblasts from 10 wg, increasing successively; acetylated SA was present from 11 wg. These findings demonstrated that changes in expression of various types of SA, occurring in human fetal skeletal muscle during early development, seem to be related to some morphofunctional aspects distinctive of this organogenesis crucial period.

Key words: Sialic acid, Skeletal muscle, Human fetus, Lectins, Immunohistochemistry

Offprint requests to: Prof. Eleonora Sgambati, Dipartimento di Bioscienze e Territorio, Università del Molise, Contrada Fonte Lappone, 86090 Pesche (Isernia), Italia. e-mail: eleonora.sgambati@unimol.it or eleonora.sgambati@live.com

DOI: 10.14670/HH-11-901

Introduction

During embryogenesis, limb musculature of vertebrates arises from precursor cells migrating from the lateral dermomyotome. The development of this migratory myogenic lineage depends on the formation of a cell precursor pool in the somite, delamination and migration to the correct target sites, and activation of the myogenic program in the limb region (Buckingham et al., 2003; Olguin et al., 2003). Among the various molecules implied in normal myogenesis and in the normal structure and functionality of the adult muscle, the sialic acids (SAs) seem to play an important role (Covault et al., 1986; Fredette et al., 1993; Brusés et al., 1995; Rafuse and Landmesser, 1996; Allan and Greer, 1998; Grow and Gordon, 2000; Hoyte et al., 2002; McDearmon et al., 2003; Suzuki et al., 2003; Johnson et al., 2004; Combs and Ervasti, 2005; Nilsson et al., 2010; Schwetz et al., 2011).

SAs are a family of large size negatively charged nine carbon 2-keto-3-deoxy sugars, frequently located in terminal position in glycan chains of many

glycoconjugates, with different structure and linkage type to the penultimate sugar acceptor. Because of these characteristics, pivotal biological functions have been proposed for the SAs, such as maintaining membrane stability and modulating various intercellular and intermolecular phenomena (Gabrielli et al., 2004; Varki, 2007; Accili et al., 2008; Schauer, 2009). The most common structural modification is the addition of one or more O-acetyl esters to hydroxyl groups (Angata and Varki, 2002; Schauer, 2004; Varki and Schauer, 2009). Linkage type can be α2-3 or α2-6 with galactose or N-acetyl-galactosamine, and α2-8 to form polysialic acid (PSA).

Studies performed on normal skeletal muscle, mostly in animal models, showed that SAs are implied in the functionality of various glycosylated molecules, involved in fiber structure, excitability, contractility and neuromuscular junction (Hoyte et al., 2002; McDearmon et al., 2003; Johnson et al., 2004; Combs and Ervasti, 2005; Nilsson et al., 2010; Schwetz et al., 2011). The role of SA in skeletal muscle has also been widely investigated, both in animal models and in human, studying the Hereditary Inclusion Body Myopathy (HIBM), a genetic pathology leading to muscular weakness and atrophy. HIBM is due to mutations of UDP-N-acetylglucosamine 2-epimerase/N-acetyl-mannosamine kinase (GNE) gene involved in SA biosynthesis (Huizing and Krasnewich, 2009). Data demonstrated that hyposialylation of glycosylated molecules, important for correct structure and functionality of skeletal muscle tissue, seems to alter their activity (Saito et al., 2004; Tajima et al., 2005; Broccolini et al., 2008, 2009, 2010, 2011; Jay et al., 2008; Broccolini et al., 2009; Huizing and Krasnewich, 2009; Jay et al., 2009; Nilsson et al., 2010; Voermans et al., 2010; Broccolini and Mirabella, 2015).

Expression changes of SA in skeletal muscle during aging were observed mostly in animal models. These seem to be related to metabolism alteration of muscle fibers (O'Connell et al., 2008) and to influence the re-innervation process, after experimental denervation (Olsen et al., 1995; Rønn et al., 2000). Our recent investigation on human skeletal muscle tissue showed expression changes of various types of SAs during aging that could be related to alterations of important molecules implied in the normal morphology and functionality of this organ (Marini et al., 2014).

To our knowledge, investigations in animal models have only been performed on the expression of SA, in particular PSA, in the skeletal muscle during embryonic and post-natal development. These studies showed that changes in expression of this anionic molecule seem to be related to differentiation and onset of the muscle functionality (Covault et al., 1986; Fredette et al., 1993; Brusés et al., 1995; Rafuse and Landmesser, 1996; Allan and Greer, 1998; Grow and Gordon, 2000; McDearmon et al., 2003; Suzuki et al., 2003). Some data, both in animals and humans, are also available in the literature, not directly on SA expression but on GNE enzyme. It seems to be essential for fetal skeletal muscle development (Krause et al., 2004; Milman et al., 2011; Daya et al., 2014).

In this study, we characterized monomeric and polymeric SAs widely and evaluated their expression in human skeletal muscle tissue from upper and lower limbs during early stages of fetal development, between 9 and 12 weeks of gestation (wg). During this period, fundamental morphofunctional events, such as secondary and mature myotubes formation, apoptosis to regulate muscle cell population, innervation, neuromuscular junction formation and contractility, occur (Fenichel, 1965; Fidziańska and Goebel, 1991; Fidziańska, 1996; Standring, 2009). Therefore, the aim of this investigation was to highlight the role of these molecules in the morphological differentiation and functionality of muscle during this developmentally crucial period.

Materials and methods

Sample collection

Specimens of upper and lower limb fetal skeletal muscle, from 9 to12 wg, were obtained from 19 pregnant women who underwent a therapeutic or voluntary abortion (9 wg n=3; 9.4 wg n=3; 9.5 wg n=2; 10 wg n=2; 10.5 wg n=2; 11 wg n=1; 11.3 wg n=2; 11.5 wg n=1; 12 wg n=3). Informed consent was obtained from each woman. The use of human fetal tissues for research purposes was approved by the Ethical Committee for investigation in humans of the Azienda Ospedaliero-Universitaria Careggi, Florence, Italy (protocol n° 6783-04). The fetal muscle samples were collected and prepared by a stereomicroscope provided with a millimetric scale.

Muscle samples were fixed in formalin solution, routinely processed, paraffin-embedded and cut in 5 μm-thick sections, for histochemical and immunohistochemical studies.

Morphofunctional changes of human skeletal muscle in early fetal development

To investigate some morphofunctional events occurring during the early development of skeletal muscle, the following stainings and methods were performed: haematoxylin-eosin, TUNEL assay, immunohistochemistry for connexin-43 and parvalbumin.

TUNEL (terminal deoxynucleotidyl transferase dUTP nick bend labeling) assay

Briefly, apoptotic cells were identified using FragelTM DNA Fragmentation Detection Kit, Fluorescent-TdT Enzym (Cat# QIA21, Calbiochem, San Diego, CA, USA). Sections from all fetal samples were deparaffinised, rehydrated and subjected to the TUNEL

assay according to the manufacturer's protocol, as previously described (Mencucci et al., 2013, 2015). The slides were evaluated and photographed using a Nikon Microphot-FXA microscope (Nikon).

Immunohistochemistry for connexin-43 and parvalbumin

Deparaffinised and rehydrated tissue sections from all fetal samples were processed using standard immunohistochemical procedures, as previously described (Mencucci et al., 2013, 2015). Briefly, sections were treated with hydrogen peroxide 3% solution for 15 minutes at room temperature to block endogenous peroxidase activity. Sections were then washed and incubated with Ultra V block (UltraVision Large Volume Detection System Anti-Polyvalent, HRP, catalogue number TP-125-HL; LabVision, Fremont, CA, USA) for 10 minutes at room temperature according to the manufacturer's protocol. After blocking non-specific site binding, slides were incubated overnight at 4°C with anti-human connexin-43 (Cx43) (1:100 dilution; Sigma-Aldrich, Saint Louis, MO, USA) and parvalbumin (1:10,000 dilution; Sigma-Aldrich) mouse monoclonal antibodies. The day after, tissue sections were rinsed in PBS and incubated with biotinylated secondary antibodies (Lab-Vision) for 10 minutes at room temperature and then with the streptavidin-biotin peroxidase (Lab-Vision) for 10 minutes at room temperature. Immunoreactivity was developed using 3,3'-diaminobenzidine tetrahydrochloride (DAB) (Sigma-Aldrich) as chromogen. All sections were treated with the same batch for each antibody to eliminate inter-batch variations. Sections not exposed to primary antibodies or incubated with isotype- and concentration-matched non-immune mouse IgG (Sigma-Aldrich) were included as negative controls for antibody specificity. The slides were evaluated and photographed using a Nikon Microphot-FXA microscope (Nikon, Tokyo, Japan).

SA expression analysis

Lectin histochemistry

Two methods for lectin histochemistry were used: the 'direct' and the 'indirect' techniques. In the 'direct' technique, *Maackia amurensis* agglutinin (MAA) and *Sambucus nigra* agglutinin (SNA) were used to identify SAs linked α2-3 and α2-6 to galactose or galactosamine, respectively (Shibuya et al., 1987; Wang et al., 1988; Gabrielli et al., 2004; Adembri et al., 2011, 2014; Marini et al., 2011, 2014). In the second method peanut agglutinin (*Arachis hypogaea*) (PNA), soybean agglutinin (*Glycine maximus*) (SBA) and *Dolichos biflorus* agglutinin (DBA) combined with neuraminidase digestion, deacetylation and differential oxidation to reveal acetylic groups, were used to investigate the expression of SAs linked to D-Gal(β1→3)-D-GalNAc, to α/βD-GalNAc >D-Gal and αD-GalNAc respectively, and the structure of SAs (Gabrielli et al., 2004; Adembri et al., 2011, 2014; Marini et al., 2011, 2014). Table 1 summarizes lectins and their specific sugar residues.

MAA and SNA were digoxigenin (DIG) labeled lectins (Roche Diagnostic, Mannheim, Germany). PNA, SBA and DBA were horseradish peroxidase (HRP) conjugated lectins (Sigma-Aldrich).

DIG-labelled lectins. The direct technique was performed as previously described (Adembri et al., 2014; Marini et al., 2014). Briefly, deparaffinised and rehydrated tissue sections from all fetal samples were treated with 20% acetic acid, to inhibit the endogenous alkaline phosphatase, then treated with 10% blocking reagent in TBS to reduce the background labelling. Afterward, sections were washed in TBS and rinsed in Buffer 1, then incubated in DIG-labelled lectins diluted in Buffer 1 (1 µL/mL and 5 µL/mL for SNA and MAA respectively) for 1 hour at room temperature. Sections were then rinsed in TBS, incubated with anti-digoxigenin conjugated with alkaline phosphatase diluted in TBS and washed in TBS. Labelling of the sites containing bound lectin-digoxigenin was obtained by incubating slides with Buffer 2, containing nitroblue tetrazolium (NBT)/X-phosphate (Roche Diagnostics, Mannheim, Germany).

HRP-conjugated lectins. The indirect technique was performed as previously described (Adembri et al., 2014; Marini et al., 2014). Briefly, deparaffinised and rehydrated tissue sections from all fetal samples were treated with 3% hydrogen peroxide to inhibit the endogenous peroxidase, rinsed in distilled water and treated with 0.1% bovine serum albumin (BSA) in TBS to reduce the background labelling. Sections were then incubated for 30 min at room temperature in HRP-conjugated lectins solution in TBS (25 µL/mL, 20 µL/mL and 25 µL/mL for PNA, SBA and DBA respectively). Then sections were rinsed in TBS. Visualization of the sites containing bound lectin-HRP was achieved by incubating slides in DAB (Sigma-Aldrich).

Enzymatic and chemical treatments. Treatments were carried out as previously performed (Adembri et al., 2014; Marini et al., 2014). Briefly, mono and polymeric SA was removed by pretreating sections for 18 hours at 37°C in a solution of sodium acetate buffer 0.25M, pH 5.5, containing 0.1 unit/ml sialidase (Type X from

Table 1. Sugar residues binding specificity of lectin.

Lectin	Abbreviation	Sugar residues binding specificity
Maackia amurensis agglutinin	MAA	Neu5Ac(α2→3)Gal
Sambucus nigra agglutinin	SNA	Neu5Ac(α2→6)Gal/GalNAc
Peanut agglutinin	PNA	D-Gal(β1→3)-D-GalNAc
Soybean agglutinin	SBA	α/β-D-GalNAc > D-Gal
Dolichos biflorus agglutinin	DBA	α-D-GalNAc

Clostridium perfringens; Sigma-Aldrich), 50mM $CaCl_2$ and 154mM NaCl, before staining with PNA, SBA and DBA. Deacetylation was performed by incubating sections with 0.5% KOH in 70% ethanol for 30 minutes at room temperature. This treatment renders SA residues, containing acetylic groups on C_4 of the pyranose ring, susceptible to neuraminidase digestion. For differential oxidation, 1 mM aqueous periodic acid (1 mM PO, mild oxidation) and 44 mM aqueous periodic acid (44 mM PO, strong oxidation) were used. Mild oxidation abolishes the staining with neuraminidase/PNA-SBA-DBA or KOH/neuraminidase/PNA-SBA-DBA when SA does not contain C_7-and/or C_8- and/or C_9-O-acetyl groups in the side-chain. Strong oxidation affects SA side-chains lacking acetyl substituents in C_9 as well as penultimate β-galactose linked via α2-6, but not if C_9 acetylated SAs linked α2-3 bound to the penultimate β-galactose are present (Gabrielli et al., 2004; Adembri et al., 2011, 2014; Marini et al., 2011, 2014).

Controls. Controls for lectin specificity included substitution of lectin-conjugates with the respective unconjugated lectins or preincubation of lectins with the corresponding hapten sugars (concentration of 0.1-0.5 M in TBS). Control of sialidase digestion was made by incubation of the sections with enzyme-free buffer. The efficacy of digestion was tested treating adjacent sections, with and without prior deacetylation, with the enzyme solution and then labeling them with MAA and SNA. Some control sections were treated with a desulfation procedure that eliminates sulfated groups present on the carbohydrate chains interfering with lectin binding (Gabrielli et al., 2004; Adembri et al., 2011, 2014; Marini et al., 2011, 2014).

PSA immunohistochemistry

Immunohistochemical technique was performed to detect PSA, as previously described (Marini et al., 2014). Briefly, endogenous peroxidase was blocked incubating the deparaffinised and rehydrated tissue sections from all fetal samples in 0.3% hydrogen peroxide for 10 min. Sections were rinsed in distilled water, treated with blocking serum for 15 min to reduce non-specific reactions and incubated with polySia-specific mAb 735 (kindly provided by Rita Gerardy-Schahn, Hannover Medical School, Hannover, Germany) (40 μg/ml in phosphate-buffered saline and 0.1% bovine serum albumin) overnight at 4°C. Then, sections were rinsed in PBS and incubated with biotinylated secondary antibodies (Lab-Vision) for 10 minutes at room temperature and then with the streptavidin-biotin peroxidase (Lab-Vision) for 10 minutes at room temperature. The development of the product was evidenced incubating sections in DAB (Sigma-Aldrich) as chromogen.

Control. Serial muscle sections were pretreated with sialidase, used also for lectin histochemistry, before staining with mAb 735 and followed the same procedure, for negative controls.

All the slides were evaluated and photographed using a Nikon Microphot-FXA microscope (Nikon, Tokyo, Japan).

Evaluation of lectin histocheistry and immunohisto-chemistry reactivity

In each section (3 sections for each specimen),10 random 600625 μm^2 optical square fields (40x objective), were examined and scored for location of lectin reactivity and immunoreactivity for Cx43, parvalbumin and PSA. In addition, two types of analyses were performed to evaluate the reactivity intensity: an arbitrary analysis (0: no reactivity; 0-1: very weak reactivity; 1: weak reactivity; 1-2: weak/moderate reactivity; 2: moderate reactivity; 2-3: moderate/strong reactivity; 3: strong reactivity; 3-4 very strong reactivity) and a quantitative analysis, measuring the average optical density (OD) on regions of interest (ROI, 40 μm^2 area) of light microscopy images, using ImageJ National Institute of Health (NIH, Bethesda, MD, USA) software. For this analysis, measured values were normalized to background [(OD-ODbkg)/ODbkg]. In each experiment, at least 8 regions of interest in 10 different optical fields were analyzed.

Statistical analysis

All values were tested for normality distribution and were expressed as mean ± standard error of the mean (SEM). Analysis of variance (ANOVA), followed by Tukey's multiple comparison test to assess differences among samples was used. Data analysis was performed using GraphPad Prism 5.0 (GraphPad Software, La Jolla, CA, USA). P values <0.05 were considered statistically significant.

Results

General morphological observations (Fig. 1)

Haematoxilyin-eosin staining showed from 9 to 10.5 wg, both in upper and lower limb, many primary myotubes surrounded by secondary myotubes and myoblasts (Fig. 1A,B); from 10 wg some secondary myotubes began to appear separate from primary ones. From 11 wg secondary myotubes increased in number and were separated from primary ones (Fig. 1C). These data are in accord with previous morphological observations on human fetal skeletal muscle (Fidziańska, 1991).

TUNEL assay (Fig. 2)

TUNEL assay demonstrated the presence of apoptotic myotubes between 9 (Fig. 2A) and 10.5 wg

(Fig. 2B) both in upper and lower limb; no apoptosis was revealed from 11 wg (Fig. 2C). The apoptotic process occurs to reduce the final number of muscle functional fibers (Fidziańska, 1996).

Immunohistochemistry and lectin histochemistry

No differences in reactivity location and intensity for immunohistochemistry and lectin histochemistry were observed in the samples between upper and lower limb, and between 9 and 9.5, 10 and 10.5, 11 and 12 wg. So, they were included in three groups as reported in table 2: group 1 (9-9.5 wg), group 2 (10-10.5 wg) and group 3 (11-12 wg).

Cx43 and parvalbumin immunoreactivity (Fig. 3)

Immunohistochemistry for Cx43, the principal protein in gap junction, showed reactivity at the plasma membrane of the myotubes, in the contact sites with myoblasts, and on the whole plasma membrane of myoblasts in group 1 (Fig. 3A). Very weak/absent reactivity in myoblasts and absent in myotubes of groups 2 and 3 was observed (Fig. 3B).

Parvalbumin immunoreactivity, cytoplasm protein binding ions Ca, involved in muscle relaxation, was detected in the cytoplasm and nucleoplasm of the myotubes with weak/moderate intensity only in group 2 (Fig. 3C,D).

Lectin reactivity location and intensity (Table 2; Figs. 4-6)

MAA and SNA. Both lectins did not react in group 1 (Table 2; Fig. 4A,D). MAA and SNA reactivity appeared in plasma membrane/basement membrane and cytoplasm of myotubes and myoblasts of group 2 (Table 2; Fig. 4B,E). Reactivity increased in group 3 (Table 2; Fig. 4C,F). Quantitative analysis showed a significantly higher intensity of reactivity in the myotubes and myoblasts of group 3 compared to group 2 ($P<0.05$) (Fig. 4G).

These reactivities indicated the appearance of monomeric SAs both linked α2-3 and α2-6 to galactose or galactosamine in group 2, increasing in group 3.

PNA and PNA with enzymatic and chemical treatments. PNA reactivity was moderate in plasma membrane/basement membrane, and very weak in cytoplasm of the myotubes and myoblasts in groups 1

Table 2. SA lectin reactivity and immunoreactivity in human fetal skeletal muscle.

	Group1 (9-9.5 wg)	Group2 (10-10.5 wg)	Group3 (11-12 wg)
MAA	0	1pm/bm 0-1c	1-2pm/bm 1c
SNA	0	1pm/bm 0-1c	1-2pm/bm 1c
PNA	2pm/bm 0-1c	2pm/bm 0-1c	1pm/bm 0-1c
Neu/PNA	3pm/bm 1c	3pm/bm 1c	3pm/bm 1c
KOH/Neu/PNA	3pm/bm 1c	3pm/bm 1c	3-4pm/bm 3c
1mMPO/Neu/PNA	2pm/bm 0-1c	2pm/bm 0-1c	2-3pm/bm 1c
1mMPO/KOH/Neu/PNA	2pm/bm 0-1c	2pm/bm 0-1c	3pm/bm 1c
44mMPO/Neu/PNA			
44mMPO/KOH/Neu/PNA	0	0	0-1
SBA	2pm/bm 1c	2pm/bm 1c	1-2pm/bm 0-1c
Neu/SBA	2pm/bm 1c	3pm/bm 1-2c	3pm/bm 2c
KOH/Neu/SBA	2pm/bm 1c	3pm/bm 1-2c	3-4pm/bm 3c
1mMPO/Neu/SBA			
1mMPO/KOH/Neu/SBA	2pm/bm 1c	2pm/bm 1c	1-2pm/bm 0-1c
44mMPO/Neu/SBA			
44mMPO/KOH/Neu/SBA	0	0	0-1
DBA	2pm/bm 1c	2pm/bm 1 c	1-2pm/bm 0-1c
Neu/DBA	2pm/bm 1c	2-3pm/bm 1-2c	2-3pm/bm 1-2c
KOH/Neu/DBA	2pm/bm 1c	2-3pm/bm 1-2c	3pm/bm 2c
1mMPO/Neu/DBA			
1mMPO/KOH/Neu/DBA	2pm/bm 1c	2pm/bm 1c	1-2pm/bm 0-1c
44mMPO/Neu/DBA			
44mMPO/KOH/Neu/DBA	0	0	0-1
polySia-specific mAb	3pm§ 1c	2pm§ 1c	0-1/0pm c

0: no reactivity; 0-1: very weak reactivity; 1: weak reactivity; 1-2: weak/moderate reactivity; 2: moderate reactivity; 2-3: moderate/strong reactivity; 3: strong reactivity; 3-4: very strong reactivity; §: 2 (group 1), 1 (group 2) in no contact sites; wg: weeks of gestation; pm: plasma membrane of myotubes and myoblasts; bm: basement membrane; c: cytoplasm of myotubes and myoblasts.

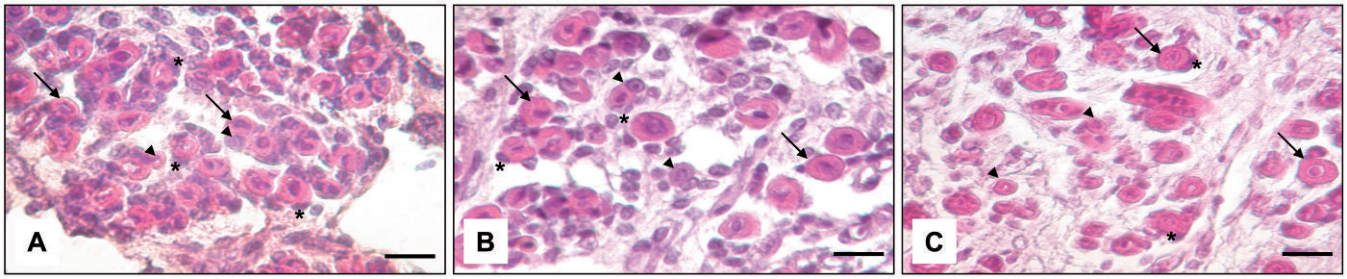

Fig. 1. Haematoxylin-eosin staining in fetal skeletal muscle. Representative micrographs of muscle samples from the lower limb of fetuses of 9.4 wg **(A)**, 10 wg **(B)** and 12 wg **(C)**. At 9.4 **(A)** and 10 **(B)** wg many primary myotubes (arrows) surrounded by secondary myotubes (arrow heads) and myoblasts (asterisks) are observable; at 10 wg some secondary myotubes are separate from primary ones. Secondary myotubes (arrows head) appear in higher number at 12 wg and are mostly separated from primary myotubes (arrows) **(C)**. Scale bar: 25 μm.

and 2 (Table 2; Fig. 5 insets A,B); in group 3 lectin reacted more weakly with respect to the other groups (Table 2; Fig. 5 inset C). After neuraminidase digestion PNA reactivity was strong in plasma membrane/basement membrane and weak in cytoplasm of the myotubes and myoblasts of groups 1, 2 and 3 (Table 2; Fig. 5A-C).

After deacetylation/neuraminidase treatment, a stronger reactivity was observed in the compartments of the myotubes and myoblasts with respect to

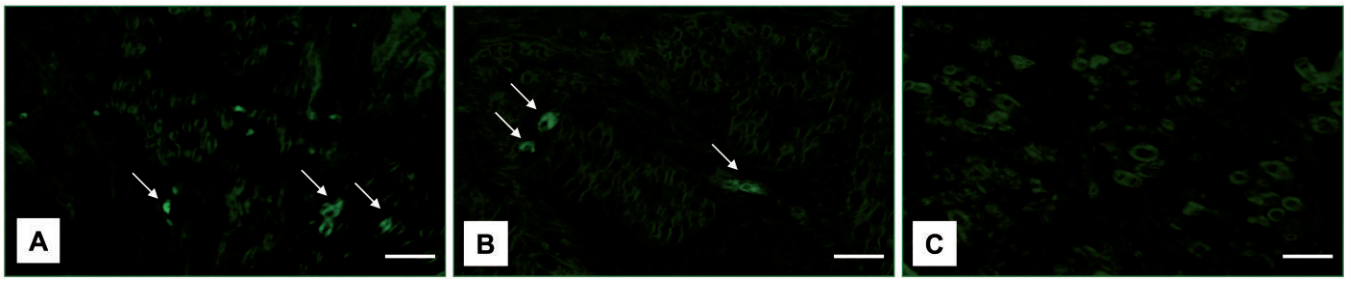

Fig. 2. TUNEL assay in fetal skeletal muscle. Representative micrographs of muscle samples from the upper limb of fetuses of 9.5 wg **(A)**, 10.5 wg **(B)** and 11.5 wg **(C)**. Apoptotic myotubes are observable at 9.5 **(A)** and 10.5 **(B)** wg (arrows); no apoptosis is visible at 11.5 wg **(C)**. Scale bar: 50 μm.

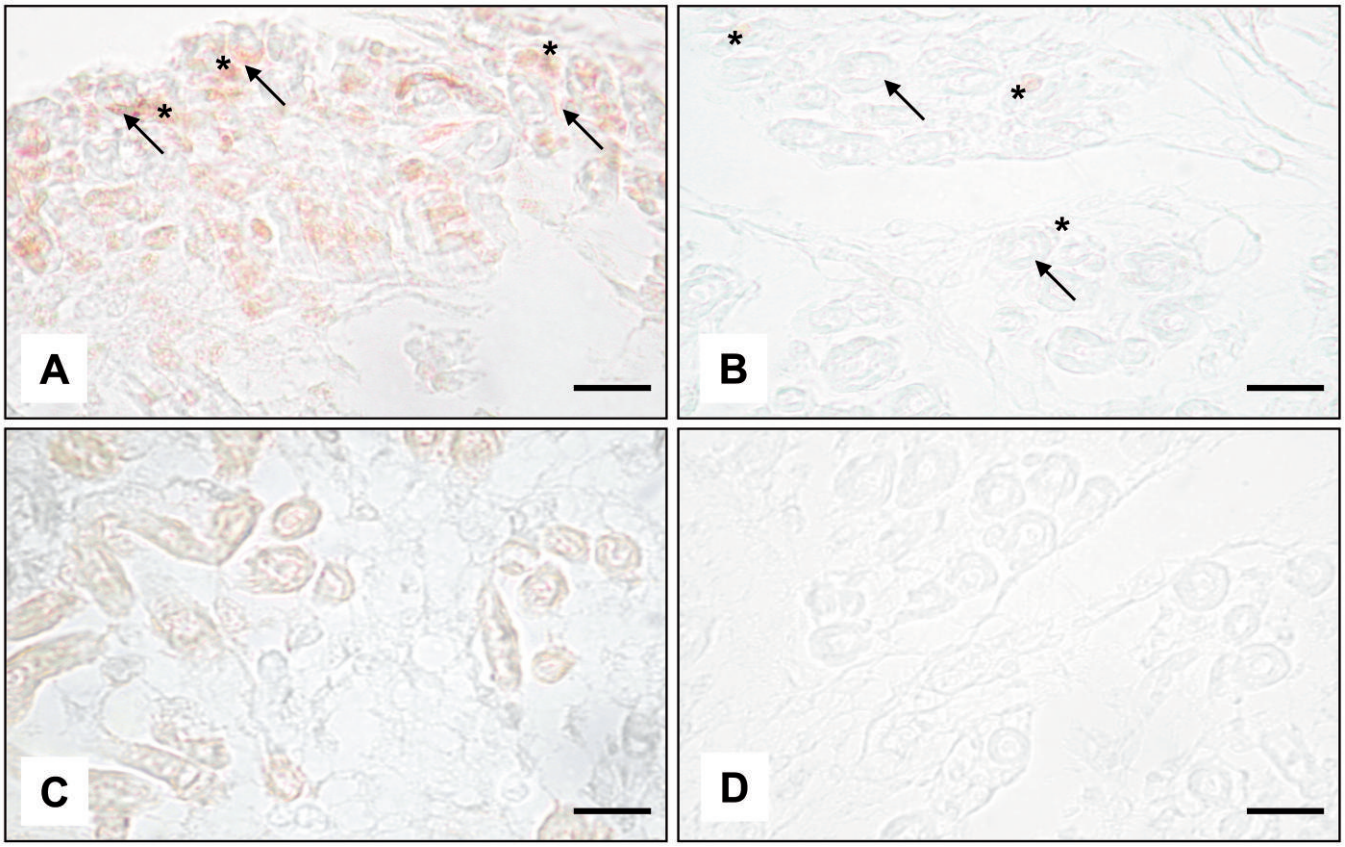

Fig. 3. Cx43 and parvalbumin immunoreactivity in fetal skeletal muscle. **A.** Representative micrograph of a group 1 muscle sample from the upper limb of fetus of 9.4 wg for Cx43. **B, D.** Representative micrograph of a group 3 muscle sample from the upper limb of fetus of 12 wg for Cx43 and parvalbumin respectively. **C.** Representative micrograph of a group 2 muscle sample from the upper limb of fetus of 10 wg for parvalbumin. Cx43 immunoreactivity is observable at the plasma membrane of the myotubes (arrows), on the contact sites with myoblasts, and on the whole plasma membrane of myoblasts (asterisks) in group 1 sample **(A)**; very weak/absent reactivity in myoblasts (asterisks), absent in myotubes (arrows) of group 3 sample is detectable **(B)**. Parvalbumin immunoreactivity is present in the cytoplasm and nucleoplasm of the myotubes with weak/moderate intensity in group 2 sample **(C)** and absent in group 3 sample **(D)**. Scale bar: 25 μm.

neuraminidase treatment only in group 3 (Table 2; Fig. 5D-F).

After mild oxidation/neuraminidase treatment, with and without deacetylation, PNA reactivity appeared the same in the compartments of myotubes and myoblasts of groups 1 and 2 compared to PNA reactivity without treatments (Table 2; Fig. 5G,H); in group 3, after mild oxidation, neuraminidase/PNA reactivity with and without deacetylation was weaker compared to neuraminidase/PNA and deacetylation/neuraminidase-PNA reactivity respectively, and stronger with respect to PNA without treatments (Table 2; Fig. 5I).

After strong oxidation/neuraminidase treatment, with and without deacetylation, absent or very weak reactivity was observed in all the muscle elements of the three groups with respect to PNA reactivity with and without other treatments (Table 2).

Quantitative analysis showed PNA reactivity significantly higher in all the myotubes/myoblasts of groups 1 and 2 with respect to group 3. After neuraminidase digestion, significantly higher reactivity intensity in the muscle elements of all groups compared to reactivity with PNA only was observed. After deacetylation/neuraminidase treatment, reactivity intensity was significantly higher in group 3 compared to groups 1 and 2, and with respect to reactivity after neuraminidase digestion only in group 3. Reactivity intensity with mild oxidation/neuraminidase/PNA, with and without deacetylation, in groups 1 and 2 appeared significantly lower with respect to neuraminidase/PNA, with and without deacetylation respectively; in group 3 mild oxidation/neuraminidase/PNA, with and without deacetylation, was lower compared to neuraminidase/PNA reactivity, with and without deacetylation respectively, and higher with respect to PNA without treatments. In addition, after mild oxidation with and without deacetylation treatment, reactivity in group 3 appeared significantly higher with respect to groups 1

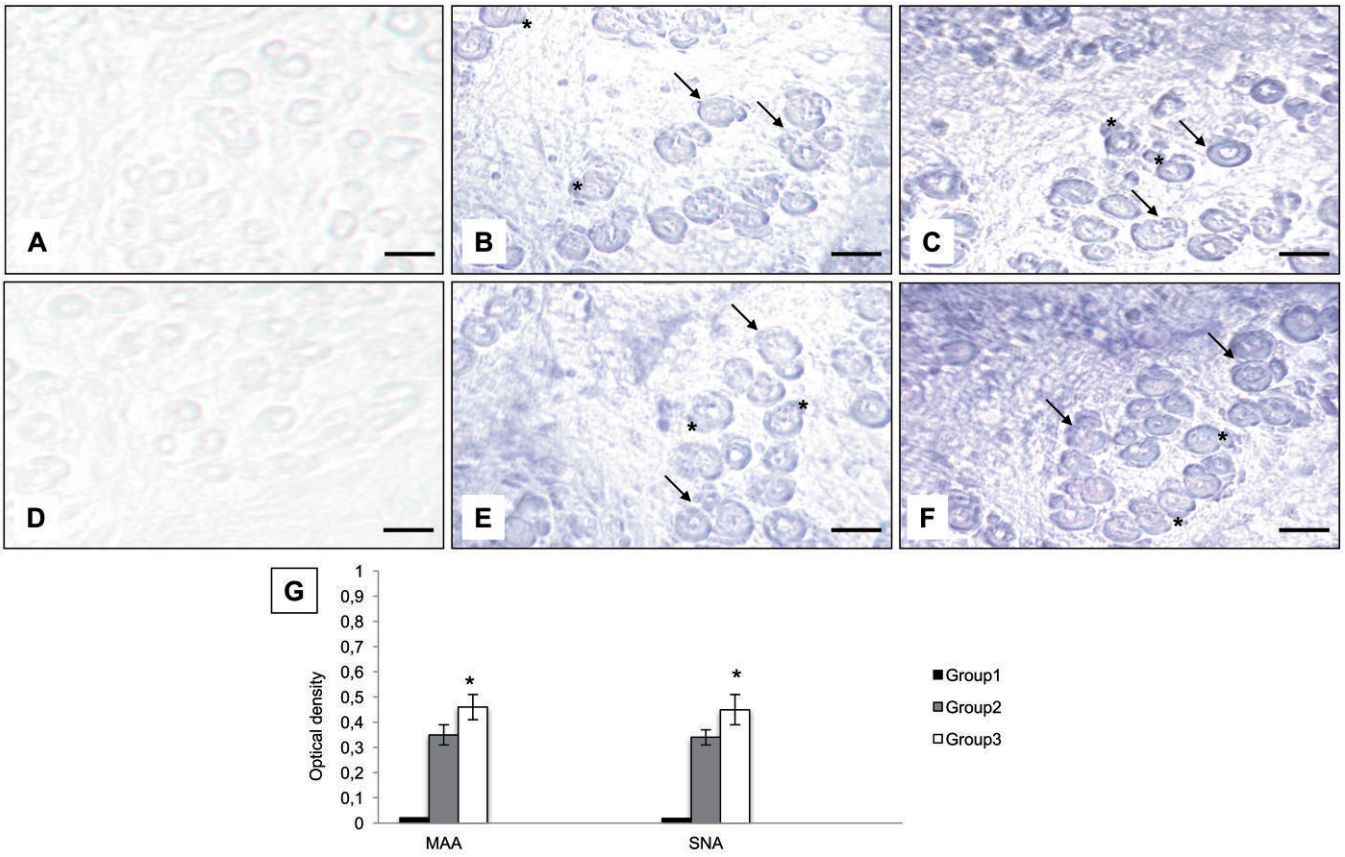

Fig. 4. MAA and SNA reactivity in fetal skeletal muscle. **A, D.** Representative micrograph of a group 1 muscle sample from the lower limb of fetus of 9.4 wg. **B, E.** Representative micrograph of a group 2 muscle sample from the lower limb of fetus of 10.5 wg. **C, F.** Representative micrograph of a group 3 muscle sample from the lower limb of fetus of 11.3 wg. **G.** Quantitative analysis in groups 1, 2 and 3 for MAA and SNA (data are the mean of OD values of all the samples in each study group). No reactivity is observable for both lectins in group 1 sample **(A) (D)**. MAA and SNA reactivity is detectable in plasma membrane/basement membrane and cytoplasm of myotubes (arrows) and myoblasts (asterisks) of group 2 samples **(B) (E)**; reactivity appears increased in group 3 **(C) (F)**. Quantitative analysis confirms that MAA and SNA reactivity intensity in myotubes/myoblasts is significantly higher in group 3 compared to group 2 **(G)** (*: $P<0.05$). Scale bar: 25 μm.

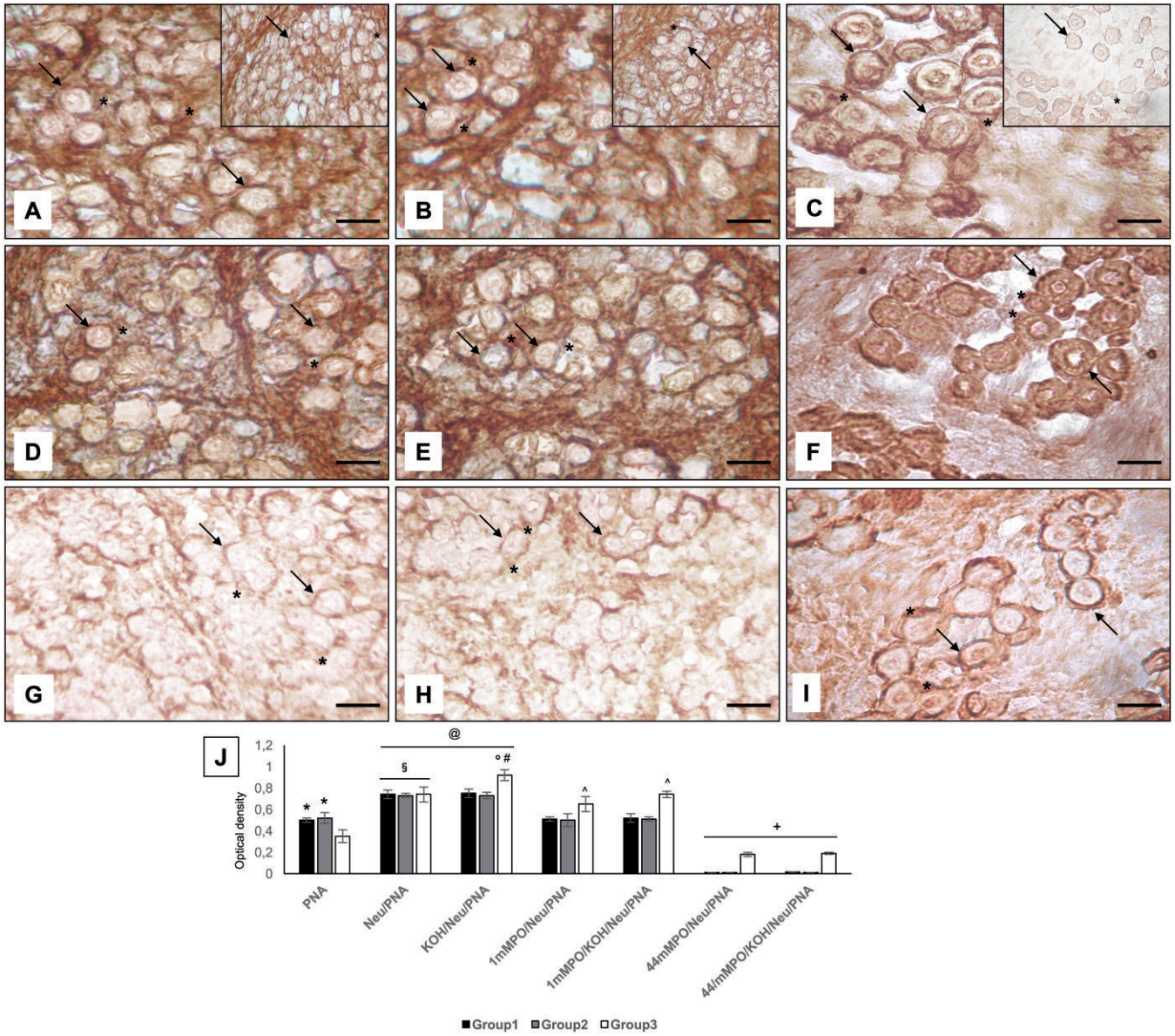

Fig. 5. PNA with and without treatments reactivity in fetal skeletal muscle. **A-C.** Neuraminidase/PNA reactivity. **Insets A-C.** PNA reactivity. **D-F.** KOH/neuraminidase/PNA reactivity. **G-I.** OD1/KOH/neuraminidase/PNA reactivity, in groups 1, 2 and 3 muscle samples from the lower limb of fetuses of 9.4, 10.5 and 11.3 wg respectively. **J.** Quantitative analysis in groups 1, 2 and 3 (data are the mean of OD values of all the samples in each study group). PNA reactivity is observable in plasma membrane/basement membrane, and in cytoplasm of the myotubes (arrows) and myoblasts (asterisks) in all the group samples (insets **A-C**); in group 3 reactivity appears weaker (inset **C**). After neuraminidase digestion PNA reactivity is stronger in all the groups **(A-C)**. After deacetylation/neuraminidase treatment, a stronger reactivity in the compartments of the myotubes (arrows) and myoblasts (asterisks) with respect to neuraminidase treatment only in group 3 is observable **(D-F)**. After mild oxidation/neuraminidase treatment, with deacetylation, PNA reactivity appears the same in the compartments of myotubes (arrows) and myoblasts (asterisks) of groups 1 and 2 compared to PNA reactivity without treatments **(G, H)**; in group 3 reactivity is weaker compared to deacetylation/neuraminidase reactivity, and stronger with respect to PNA without treatments **(I)**. Quantitative analysis **(J)** shows PNA reactivity significantly higher in all the myotubes/myoblasts of groups 1 and 2 with respect to group 3 (*: P<0.05). After neuraminidase digestion, a significantly higher reactivity intensity in the muscle elements of all groups is shown compared to reactivity with PNA only (§: P<0.05). After deacetylation/neuraminidase treatment, reactivity intensity is significantly higher in group 3 compared to groups 1 and 2 (°: P<0.05) and, with respect to reactivity after neuraminidase digestion, only in group 3 (#: P<0.05). Reactivity intensity with neuraminidase/PNA and deacetylation-neuraminidase/PNA in groups 1, 2 and 3 is significantly higher with respect to mild oxidation/neuraminidase/PNA, with and without deacetylation (@: P<0.05); in group 3 mild oxidation/PNA reactivity intensity, with and without deacetylation, is higher with respect to that in groups 1 and 2 and compared to PNA reactivity without treatments in group 3 (^: P<0.05). Strong oxidation/neuraminidase/PNA reactivity (with and without deacetylation) is significantly lower compared to all the other treatments and without treatments in both groups (+: P<0.05). Scale bar: A, B, D, E, G, H, 25 μm; C, F, I, 20 μm; insets A-C, 60 μm.

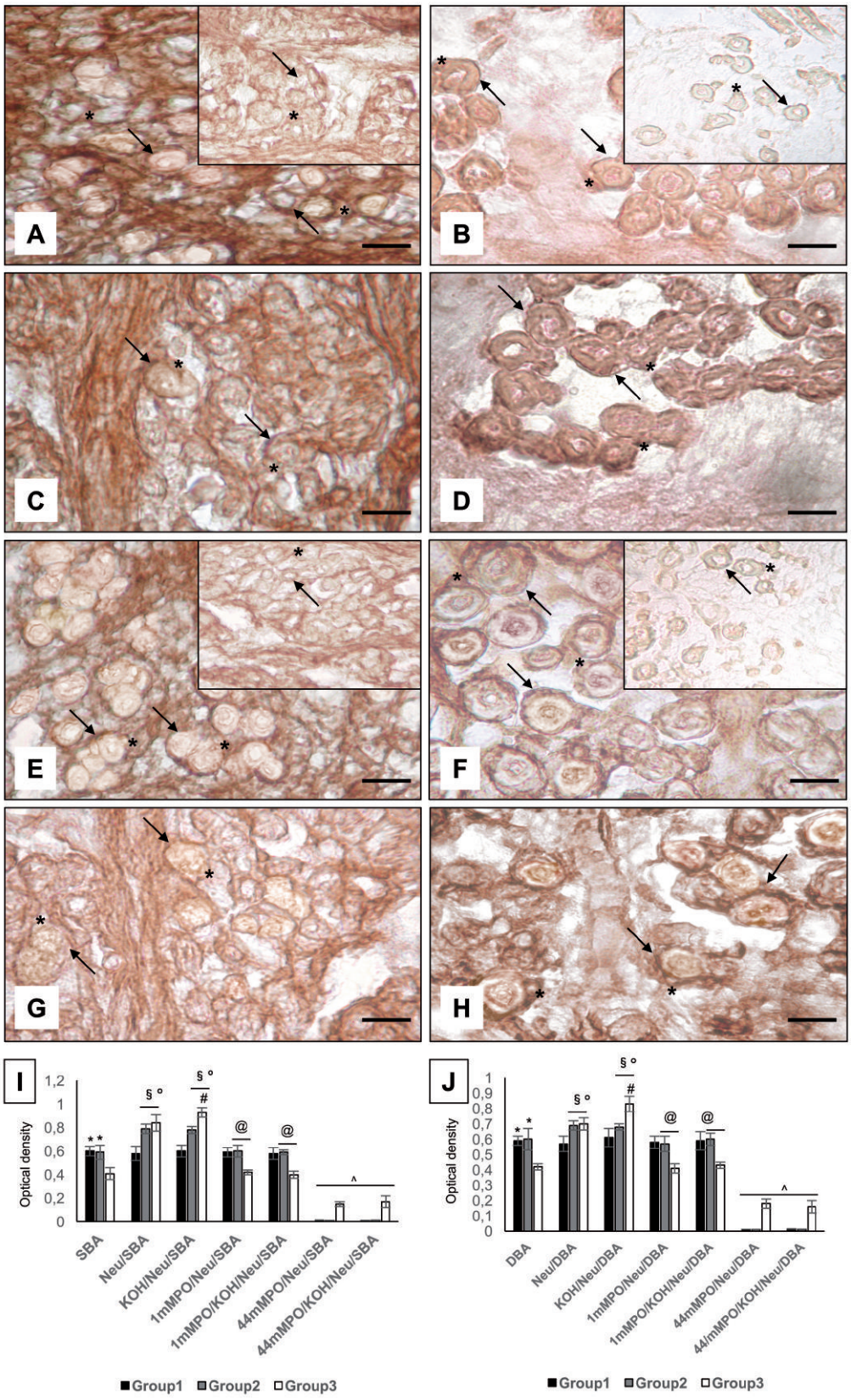

Fig. 6. SBA and DBA with and without treatments reactivity in fetal skeletal muscle. **A, B.** Neuraminidase/SBA reactivity. **Insets A, B.** SBA reactivity. **C, D.** KOH/neuraminidase/SBA reactivity. **E, F.** Neuraminidase/DBA reactivity. **Insets E, F.** DBA reactivity. **G, H.** KOH/neuraminidase/DBA reactivity, in groups 2 and 3 muscle samples from the lower limb of fetuses of 10.5 and 11.3 wg respectively. **I, J.** Quantitative analysis in groups 1, 2 and 3 for SBA and DBA respectively (data are the mean of OD values of all the samples in each study group). SBA (insets **A, B**) and DBA (insets **E, F**) reactivity is observable in plasma membrane/basement membrane and in cytoplasm of myotubes (arrows) and myoblasts (asterisks) of groups 2 and 3 samples; reactivity is weaker in group 3. After neuraminidase digestion, SBA **(A, B)** and DBA **(E, F)** reactivity appears stronger in myotubes (arrows) and myoblasts (asterisks) of groups 2 and 3, compared to SBA and DBA reactivity; only in group 3 a stronger reactivity is observable after neuraminidase treatment with deacetylation compared to without deacetylation **(C, D, G, H)**. Quantitative analysis shows statistically significant higher SBA **(I)** and DBA **(J)** reactivity in the myotubes/myoblasts of groups 1 and 2 with respect to group 3 (*: $P<0.05$). Significantly higher reactivity intensity is observable after neuraminidase treatment with and without deacetylation in all the muscle elements of groups 2 and 3 with respect to reactivity with SBA and DBA only (§: $P<0.05$), and in the same groups compared to group 1 (°: $P<0.05$); in group 3, after neuraminidase treatment with deacetylation, reactivity is significantly higher compared to that without deacetylation (#: $P<0.05$). Reactivity intensity of mild oxidation/neuraminidase/SBA-DBA, with and without deacetylation, is significantly lower with respect to neuraminidase/SBA-DBA, with and without deacetylation respectively, in all the muscle elements of groups 2 and 3 (@: $P<0.05$). Strong oxidation/neuraminidase/SBA-DBA reactivity (with and without deacetylation) is significantly lower compared to all the other treatments and without treatments in all the groups (^: $P<0.05$). Scale bar: A, C, E, G, 25 μm; B, D, F, H, 20 μm; insets A, B, E, F, 60 µm.

and 2. Strong oxidation/neuraminidase/PNA reactivity (with and without deacetylation) was significantly lower compared to all the other treatments and without treatments in all the groups ($P<0.05$) (Fig. 5J).

Altogether, the results of PNA reactivity indicated the presence of SA linked to D-Gal(β1→3)-D-GalNAc in groups 1 and 2, increasing in group 3. In addition, SA acetylated in C4, in C7 and/or C8 and/or C9 linked via α2-6 was present in group 3 only.

SBA and DBA, SBA and DBA with enzymatic and chemical treatments. SBA and DBA reactivity was moderate in plasma membrane/basement membrane and weak in cytoplasm of myoblasts/myotubes in groups 1 and 2 (Table 2; Fig. 6 insets A,E); reactivity was weaker in group 3 (Table 2; Fig. 6 insets B,F). After neuraminidase digestion, SBA and DBA reactivity was stronger in all the muscle compartments of groups 2 and 3 (Table 2; Fig. 6A,B,E,F); only in group 3 a stronger reactivity was observed after neuraminidase treatment with deacetylation compared to treatment without deacetylation (Table 2; Fig. 6C,D,G,H).

After mild oxidation/neuraminidase treatments, with and without deacetylation, the same reactivity was detected in myotubes/myoblasts of group 1 with respect to reactivity with lectins without treatments or with the other treatments; in groups 2 and 3, after mild oxidation/neuraminidase treatments reactivity was the same with respect to lectins without treatments, but weaker with respect to the other treatments (Table 2). Strong oxidation treatment, with and without deacetylation, abolished or strongly decreased the reactivity in all the components of the three groups (Table 2).

Quantitative analysis showed statistically significant higher SBA and DBA reactivity in all the myotubes/myoblasts in groups 1 and 2 with respect to group 3. Significantly higher reactivity intensity was also observed after neuraminidase treatment with and without deacetylation in the muscle elements of groups 2 and 3 with respect to reactivity with SBA and DBA only, and in the same groups compared to group 1. In group 3, after neuraminidase treatment with deacetylation, reactivity was significantly higher with respect to that without deacetylation. In all the muscle elements of groups 2 and 3, mild oxidation/neuraminidase/SBA-DBA reactivity intensity, with and without deacetylation, appeared significantly lower with respect to neuraminidase/SBA-DBA respectively, with and without deacetylation ($P<0.05$). Strong oxidation/neuraminidase/PNA reactivity (with and without deacetylation) was significantly lower compared to all the other treatments and without treatments in all the groups ($P<0.05$) (Fig. I, J).

Overall, the results of SBA and DBA reactivity indicated the presence of SA linked to α and β D-GalNAc in group 2 and, more abundant, in group 3; acetylated SA in C4 was present only in group 3. C7 and/or C8 and/or C9 acetylic group in SA were absent in all the groups.

Controls. Sections incubated with lectins and their corresponding hapten sugars and sections incubated with unconjugated lectins, were unstained. Sections incubated

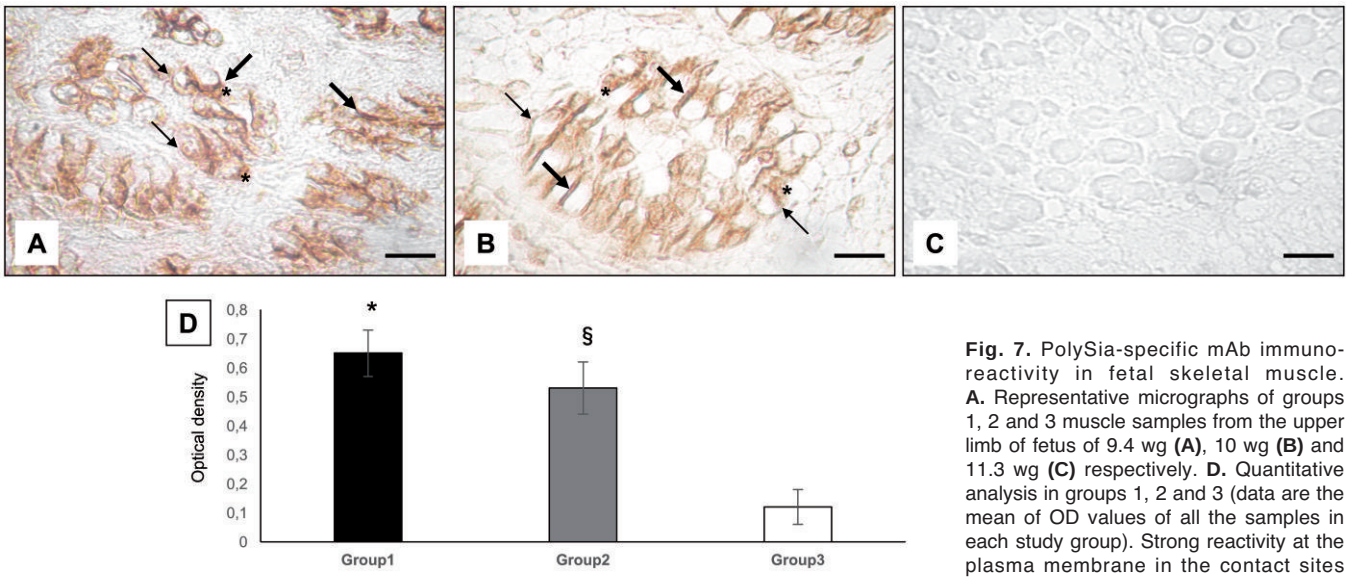

Fig. 7. PolySia-specific mAb immunoreactivity in fetal skeletal muscle. **A.** Representative micrographs of groups 1, 2 and 3 muscle samples from the upper limb of fetus of 9.4 wg **(A)**, 10 wg **(B)** and 11.3 wg **(C)** respectively. **D.** Quantitative analysis in groups 1, 2 and 3 (data are the mean of OD values of all the samples in each study group). Strong reactivity at the plasma membrane in the contact sites (thick arrows), moderate in the no contact sites (thin arrows) and weak in cytoplasm of myotubes and myoblasts (asterisks) in the group 1 sample **(A)** is observable; weaker reactivity in myotubes and myoblasts, both in contact (thick arrows) and no contact sites (thin arrows) is detectable in group 2 sample **(B)**; in group 3 sample no reactivity is visible **(C)**. Quantitative analysis confirms significantly higher reactivity intensity in myotubes/myoblasts of group1 with respect to groups 2 and 3 (*: $P<0.05$), and in group 2 compared to group 3 (§: $P<0.05$) **(D)**. Scale bar: 25μm.

with enzyme-free buffer did not show any change in lectin binding. Results of the efficacy of enzymatic digestion were as expected. Desulfation procedure did not prove to affect the subsequent lectin binding (data not shown).

Location and intensity of polySia-specific mAb immunoreactivity (Table 2; Fig. 7)

Immunohistochemistry for PSA showed strong reactivity at the plasma membrane in the contact sites, moderate in the no contact sites and weak in cytoplasm of all myotubes and myoblasts, in group 1 (Table 2; Fig. 7A). Weaker reactivity in myotubes and myoblasts was observed in group 2 (Table 2; Fig 7B). In group 3 very weak or absent reactivity was seen (Table 2; Fig 7C). Quantitative analysis showed a significant lower reactivity intensity in groups 2 and 3 with respect to group 1 and in group 3 compared to group 2 ($P<0.05$) (Fig. 7D).

The results indicated presence of PSA in myoblast and myotubes in groups 1 and 2, drastically decreased or disappeared in group 3.

Controls. Sections pretreated with sialidase before staining with mAb 735 showed no reactivity (data not shown).

Discussion

The present investigation showed for the first time that changes in distribution and content of different types of SAs in human fetal skeletal muscle tissue occur in limb early myogenesis during a key development period, comprised between 9 and 12 wg. We also demonstrated that changes of some morphofunctional aspects such as apoptosis, cell interaction, contractility-relaxation and cell growth, seem to be associated with these differences in SA expression.

Our findings, arising from lectin direct method, demonstrated the appearance of monomeric SAs linked α2-3 to galactose (MAA) and α2-6 to galactose and/or galactosamine (SNA), in plasma membrane/basement membrane and cytoplasm of the myoblasts and myotubes from 10 wg, increasing in the following ones. Lectin indirect method with neuraminidase and chemical treatments confirmed the presence of SAs linked to galactose and galactosamine, in particular to D-Gal(β1→3)-D-GalNAc (PNA), to α and β D-GalNAc (SBA) and to α D-GalNAc (DBA), in plasma membrane/basement membrane and cytoplasm of the muscle elements from 10 wg. It is to be noted that SA linked to D-Gal(β1→3)-D-GalNAc (PNA) was also present from 9 wg in the plasma membrane/basement membrane and cytoplasm of myotubes and myoblasts. This is explained by the fact that PNA reactivity after neuraminidase treatment can indicate indirectly also the presence of PSA, as neuraminidase used in our experiments removes SAs linked not only α2-3 and α2-6 but also α-2,8 (Marini et al., 2014). In addition, PSA chain is mostly "primed" on an initiating SA residue linked α2-3 to galactose (Varki and Schauer, 2009). The apparent presence of PSA in basement membrane is due to the fact that it is attached to the glycoprotein neural cell adhesion molecule (NCAM), forming the complex PSA-NCAM mostly, and projects into the extracellular matrix. The presence of PSA in plasma membrane, in particular in contact sites, and in cytoplasm of myotubes and myoblasts from 9 to 9.5 wg was confirmed by immunohistochemistry. From 10 to 10.5 wg PSA begins to decrease and from 11 to 12 wg it is drastically reduced or disappeared in all muscle elements. Another noteworthy finding is the presence of acetylated SAs, in particular those linked to galactose, but only from 11 to 12 wg. Therefore, PSA is present in early stages of examined development period of muscle and decreases/disappears with appearance of monomeric SAs, which change their structure in a short time.

Regarding morphofunctional changes investigated in this study, we observed: i) apoptotic myotubes were more evident between 9 and 10.5 wg, disappearing from 11 wg; ii) Cx43 was more abundant between 9 and 9.5 wg in myotubes and myoblasts and particularly in contact sites, drastically decreasing and/or disappearing from 10 wg; iii) parvalbumin was present in cytoplasm and nucleoplasm of myotubes only between 10 and 10.5 wg.

It is known that PSA is in general overexpressed during rat muscle development and decreases after postnatal development (Olsen et al., 1995; Rønn et al., 2000). In particular, studies on animal models *in vivo* and *in vitro* showed that PSA is transiently up-regulated on myotubes undergoing separation during both primary and secondary myogenesis, and is restricted to those regions of primary and secondary myotube plasma membrane, which are juxtaposed and about to separate. This separation provides a signal to stop further myoblast fusion too (Fredette et al., 1993; Allan and Greer, 1998). It is to be kept in mind that not sialylated NCAM seems to be involved in the beginning of myoblast fusion (Suzuki et al., 2003). In addition, PSA-NCAM is highly expressed also by axons throughout nerve outgrowth up to its down-regulation once the mature intramuscular branching pattern occurs and secondary myogenesis is complete (Brusés et al., 1995; Allan and Greer, 1998). It is interesting the hypothesis that the close proximity of axons to newly forming myotubes implicates axon-myotube communication in triggering myotube formation and PSA-NCAM expression (Allan and Greer, 1998). This is supported by the demonstration that neuromuscular electrical activity and myotube contractility positively regulate myotube expression of PSA-NCAM in a mechanism involving an influx of calcium and activation of protein kinase C (Fredette et al., 1993; Rafuse and Landmesser, 1996). Alternatively, physical contact between developing myotubes could also be intimately correlated with PSA-NCAM labelling, with the expression on primary and secondary myotubes commencing upon initial contact

and declining after separation. This contact-related control may be mediated by a combination of inter-myotube gap junctional communication, contact-stimulated myotube surface receptor activity and/or nerve-induced contractile activity (Allan and Greer, 1998). PSA on myotubes may even concentrate the fibroblast growth factor (FGF) and present it to its receptor, stopping myoblast fusion. It is known that FGF inhibits myoblasts fusion (Suzuki et al., 2003). Our findings on PSA partially adhere to those in the literature: the presence of this molecule was observed, although in smaller amount, in myotubes in the no contact sites and in myoblasts too. In addition, it is noteworthy that from 10 wg Cx43 drastically diminishes, while parvalbumin appears, disappearing afterwards suddenly in cytoplasm and nucleoplasm of myotubes. Several studies, always in animal models, demonstrated that Cx43 is the principal gap junction protein and plays an important role in transferring signals involved in correct myogenetic events, such as fusion of myoblasts and coordinated maturation of contractile capabilities (Araya et al., 2003, 2005; Anderson et al., 2006; Gorbe et al., 2007; von Maltzahn et al., 2011). It has been shown that parvalbumin is a relaxation factor in the postnatal muscle, particularly in animals, acting as a shuttle to the transfer of Ca^{2+} from myofibrils to the cytoplasmic reticulum (Berchtold et al., 2000; Murphy et al., 2012). Ca^{2+} is present also in the nucleoplasm of every type of cell, and plays specific biological effects such as activation of distinct genes, transcription factors and intranuclear kinases and regulation of cell growth (Resende et al., 2013). In addition, parvalbumin has been used as a molecular tool buffering intracellular Ca^{2+} to demonstrate that in nucleoplasm decrease of Ca^{2+} slows cell growth (Resende et al., 2013).

Altogether our results could indicate that a period of isolation, of contractility stop and changes in various biological processes in muscle elements occurs from 10 to 10.5 wg, in order to prepare for future morpho-functional events, such as new innervation and/or redistribution of nervous branching (already began about at 8 wg), maturation of myofibrillar apparatus and other maturative processes, leading to mature myotubes.

No data is present in the literature regarding monoSA expression in embryonic skeletal muscle tissue. Several investigations demonstrated in muscle cell cultures and muscle adult normal and HIBM tissue the importance of SA in functionality of skeletal muscle glycoproteins such as α-dystroglycan and neprilysin. The α-dystroglycan is a dystroglycan complex glycoprotein, component of the dystrophin-glycoprotein complex located in the sarcolemma of striated muscle fibers. α-dystroglycan, binding to several extracellular ligands, seems to play an important role in mechanical protection of the sarcolemma against shear stresses imposed during muscle contraction and in maintaining sarcolemma integrity (Combs and Ervasti, 2005; Nilsson et al., 2010). In addition, of note, SA in α -dystroglycan seems to have a role in laminin-induced AChR (acetylcholine receptor) clustering in neuromuscular junctions (McDearmon et al., 2003). Neprilysin (NEP) is a richly sialylated metallopeptidase of plasma membrane that cleaves amyloid-β (Aβ) in various sites (Broccolini and Mirabella, 2015). Moreover, neprilysin appears to play in skeletal muscle a role during development/regeneration, cleaving the insulin-like growth factor-I (IGF-I) binding protein 5, thus modulating IGF-I/Akt cellular survival pathway (Broccolini et al., 2006). It is noteworthy that NEP is overexpressed during myotubes formation, decreasing in those mature at the end of the differentiation processes (Broccolini et al., 2006). In HIBM pathology it has been supposed that hyposialylation would impair neprilysin stability and enzymatic function, favoring the progressive degenerative process of muscle fibers (Broccolini et al., 2008, 2009, 2011; Jay et al., 2009; Malicdan et al., 2009; Broccolini and Mirabella, 2015). The presence of SA on other glycoproteic complex molecules, determinant for muscle excitability, such as voltage-gated sodium and potassium channels, was demonstrated to be important for their activity modulation (Johnson et al., 2004; Jay et al., 2009; Schwetz et al., 2011). SA may have an important role in several other muscle glycoproteins too, for example in conferring stability and acting as scavenger of free radicals (Saito et al., 2004; Huizing and Krasnewich, 2009; Malicdan et al., 2009). Other investigations reported that the presence of SA in the glycocalyx of the plasma membrane is necessary to prevent uncontrolled entry of calcium into fibers (Jay et al., 2008, 2009). In addition, gangliosides, richly sialylated glycolipids, seem to be involved in regulation of numerous cellular pathways in skeletal muscle, such as proliferation, differentiation, hormone response, trophic effect and control of apoptosis (Bruni and Donati, 2008; Paccalet et al., 2010).

In view of the literature data, our findings on the appearance and distribution of various monoSA types, when probably a period of isolation, of contractility stop and changes in cell biological processes occur, could suggest their importance in the formation of functional molecular complexes essential to complete the proper human myogenesis and to prepare the muscle to a correct functionality. It is noteworthy that from 11 wg, when human mature myotubes are forming and apoptosis is not more evident, besides an increase of SAs, their sudden acetylation occurs. Some investigations showed that acetylated SAs seem to have important functions in embryogenesis, development, immunological processes and in the regulation of ganglioside-mediated apoptosis (Chen and Varki, 2002; Malisan et al., 2002; Mandal et al., 2015). It has been also seen that acetylation of different proteins could protect from apoptosis through the Akt survival pathway and controlling multiple apoptotic mediators (Yi et al., 2011; Zacharias et al., 2011). We can speculate that acetylation in fetal muscle could have a role in stabilizing the structure of various sialylated molecules, promoting their correct functions, and protecting against

apoptotic stimuli.

Another interesting finding arising from our study regards the same appearance time and the same expression of the various types of monoSAs in basement membrane surrounding myotubes and myoblasts from 10 wg. Investigations on basement membrane in fetal skeletal muscle, well developed from 11 wg (Fidziańska and Goebel, 1991), demonstrated the important role of this structure in various biological processes: scaffold for promoting myogenesis and synaptogenesis, elastic sheath around myotubes/myoblasts, improving plasma membrane stability, assembly neuromuscular and myotendineous areas, concentring growth factors for myogenesis and probably many other processes (Campbell and Stull, 2003; Sanes, 2003; Yurchenco, 2011). The components of basements that play a key role in these functions are various glycoproteins and proteoglycans such as laminin, fibronectin, collagen, perlecan, agrin. Therefore, SA components in all or some of these molecules could be essential for their functionality. It is not excluded that acetylated SAs may also play a role in basement membrane as a barrier for extracellular apoptotic stimuli.

It is even to be kept in mind that some enzymatic complexes are involved in SAs synthesis, transfer on carbohydrate chain, addition of acetylic groups and degradation (Krause et al., 2004; Varki and Schauer, 2009; Fanzani et al., 2012). In particular, investigations on human myoblasts cell culture and on animal models muscle tissue during myogenesis, modulation of GNE (regulating sialyltransferases, in SA biosynthesis) and sialidases have been demonstrated to be implied in various processes, such as muscle integrity and activity, myofiber development and sarcomere organization and apoptosis (Krause et al., 2004; Milman Krentsis et al., 2011; Fanzani et al., 2012; Daya et al., 2014). The action of these enzymatic complexes seems to be strictly correlated to that of myogenic factors (Anastasia et al. 2008; Milman Krentsis et al., 2011; Fanzani et al., 2012; Daya et al., 2014). A functional inter-correlation between SAs and myogenic factors during myogenesis can be supposed, too. In future studies, it could be interesting to investigate the expression of enzymatic complexes and myogenic factors during the same development period of human skeletal muscle examined in the present study, to understand better the mechanisms at the basis of myogenesis.

In conclusion, our findings showed changes in the expression of the various types of SA investigated during a short but important period of myogenesis. In particular, PSA seems to determine separation and isolation of myotubes and myoblasts to permit future and correct muscle maturation. When PSA is disappearing, monomeric SAs appearance, increase and changes in structure (acetylation) could be implied in functionality of molecular complexes important to lead towards a complete and correct myogenesis. Sialylation changes in various molecules during early stages of development could contribute to altered myogenesis leading to HIBM pathology (due to GNE gene mutation) but also to other congenital myopathies whose causes are still not well known (North et al., 2014).

References

Accili D., Menghi G. and Gabrielli M.G. (2008). Lectin histochemistry for in situ profiling of rat colon sialoglycoconjugates. Histol. Histopathol. 23, 863-875.

Adembri C., Selmi V., Vitali L., Nosi D., Tani A., Zappoli Thyrion G.D., Santoro G., Bonaccini L., Avveduto G., Caldini A.L. and Sgambati E. (2014). Expression and characterization of anionic components in the tubulointerstitial compartment of rat kidney during polymicrobial sepsis. Acta histochem. 116, 94-105.

Adembri C., Sgambati E., Vitali L., Selmi V., Margheri M., Tani A., Bonaccini L., Nosi D., Caldini A.L., Formigli L. and De Gaudio A.R. (2011). Sepsis induces albuminuria and alterations in the glomerular filtration barrier: a morphofunctional study in the rat. Crit. Care 15, R277.

Allan D.W. and Greer J.L. (1998). Polysialylated NCAM expression during motor axon outgrowth and myogenesis in the fetal rat. J. Comp. Neurol. 391, 275-292.

Anastasia L., Papini N., Colazzo F., Palazzolo G., Tringali C., Dileo L., Piccoli M., Conforti E., Sitzia C., Monti E., Sampaolesi M., Tettamanti G. and Venerando B. (2008). NEU3 Sialidase strictly modulates GM3 levels in skeletal myoblasts C2C12 thus favoring their differentiation and protecting them from apoptosis. J. Biol. Chem. 283, 36265-36271.

Anderson C., Catoe H. and Werner R. (2006). MIR-206 regulates connexin43 expression during skeletal muscle development. Nucleic Acids Res. 34, 5863-5871.

Angata T. and Varki A. (2002). Chemical diversity in the sialic acids and related alpha-keto acids: an evolutionary perspective. Chem. Rev. 102, 439-470.

Araya R., Eckardt D., Riquelme M.A., Willecke K. and Sáez J.C. (2003). Presence and importance of connexin43 during myogenesis. Cell Commun. Adhes. 10, 451-456.

Araya R., Eckardt D., Maxeiner S., Krüger O., Theis M., Willecke K. and Sáez J.C. (2005). Expression of connexins during differentiation and regeneration of skeletal muscle: functional relevance of connexin43. J. Cell Sci. 118, 27-37.

Berchtold M.W., Brinkmeier H. and Müntener M. (2000). Calcium ion in skeletal muscle: its crucial role for muscle function, plasticity, and disease. Physiol. Rev. 80, 1215-1265.

Broccolini A. and Mirabella M. (2015). Hereditary inclusion-body myopathies. Biochim. Biophys. Acta 1852, 644-650.

Broccolini A., Gidaro T., Morosetti R., Gliubizzi C., Servidei T., Pescatori M., Tonali P.A., Ricci E. and Mirabella M. (2006). Neprilysin participates in skeletal muscle regeneration and is accumulated in abnormal muscle fibres of inclusion body myositis. J. Neurochem. 96, 777-789.

Broccolini A., Gidaro T., De Cristofaro R., Morosetti R., Gliubizzi C., Ricci E., Tonali P.A. and Mirabella M. (2008). Hyposialylation of neprilysin possibly affects its expression and enzymatic activity in hereditary inclusion-body myopathy muscle. J. Neurochem. 105, 971-981.

Broccolini A., Gidaro T., Morosetti R. and Mirabella M. (2009). Hereditary inclusion-body myopathy: clues on pathogenesis and possible therapy. Muscle Nerve 40, 340-349.

Broccolini A., Gidaro T., Tasca G., Morosetti R., Rodolico C., Ricci E. and Mirabella M. (2010). Analysis of NCAM helps identify unusual phenotypes of hereditary inclusion-body myopathy. Neurology 75, 265-272.

Broccolini A., Gidaro T., Morosetti R., Sancricca C. and Mirabella M. (2011). Hereditary inclusion-body myopathy with sparing of the quadriceps: the many tiles of an incomplete puzzle. Acta Myol. 30, 91-95.

Bruni P. and Donati C. (2008). Pleiotropic effects of sphingolipids in skeletal muscle. Cell Mol. Life Sci. 65, 3725-3736.

Brusés J.L., Oka S. and Rutishauser U. (1995). NCAM-associated polysialic acid on ciliary ganglion neurons is regulated by polysialytransferase levels and interaction with muscle. J. Neurosci. 15, 8310-8319.

Buckingham M., Bajard L., Chang T., Daubas P., Hadchouel J., Meilhac S., Montarras D., Rocancourt D. and Frédéric Relaix. (2003). The formation of skeletal muscle: from somite to limb. J. Anat. 202, 59-68.

Campbell K.P. and Stull J.T. (2003). Skeletal muscle basement membrane-sarcolemma-cytoskeleton interaction. J. Biol. Chem. 278, 12599-12600.

Chen H.Y. and Varki A. (2002). O-acetylation of GD3: an enigmatic modification regulating apoptosis? J. Exp. Med. 196, 1529-1533.

Combs A.C. and Ervasti J.M. (2005). Enhanced laminin binding by alpha-dystroglycan after enzymatic deglycosylation. Biochem. J. 390, 303-309.

Covault J., Merlie J.P., Goridis C. and Sanes J.R. (1986). Molecular forms of N-CAM and its RNA in developing and denervated skeletal muscle. J. Cell Biol. 102, 731-739.

Daya A., Vatine G.D., Becker-Cohen M., Tal-Goldberg T., Friedmann A., Gothilf Y., Jun Du S. and Mitrani-Rosenbaum S. (2014). Gne depletion during zebrafish development impairs skeletal muscle structure and function. Hum. Mol. Genet. 23, 3349-3361.

Fanzani A., Zanola A., Faggi F., Papini N., Venerando B., Tettamanti G., Sampaolesi M. and Monti E. (2012). Implications for the mammalian sialidases in the physiopathology of skeletal muscle. Skelet. Muscle 2, 23.

Fenichel G.M. (1965). The development of human skeletal muscle. Dev. Med. Child Neurol. 7, 69-72.

Fidziańska A. and Goebel H.H. (1991). Human ontogenesis. 3. Cell death in fetal muscle. Acta Neuropathol. 8, 572-577.

Fidziańska A. (1996). Apoptosis in human embryonic and diseased skeletal muscle. Basic Appl. Myol. 6, 261-264.

Fredette B., Rutishauser U. and Landmesser L. (1993). Regulation and activity-dependence of N-Cadherin, NCAM isoforms, and polysialic acid on chick myotubes during development. J. Cell Biol. 123, 1867-1888.

Gabrielli M.G., Bondi A.M., Materazzi G. and Menghi G. (2004). Differential location and structural specificities of sialic acid-beta-D-Gal sequences belonging to sialoderivatives of rabbit oviduct under hormonal treatment. Histol Histopathol 19, 1175-1186.

Gorbe A., Krenacs T., Cook J.E. and Becker D.L. (2007). Myoblast proliferation and syncytial fusion both depend on connexin43 function in transfected skeletal muscle primary cultures. Exp. Cell Res. 313, 1135-1148.

Grow W.A. and Gordon H. (2000). Sialic acid inhibits agrin signaling in C2 myotubes. Cell Tissue Res. 299, 273-279.

Hoyte K., Kang C. and Martin P.T. (2002). Definition of pre- and postsynaptic forms of the CT carbohydrate antigen at the neuromuscular junction: ubiquitous expression of the CT antigens and the CT GalNAc transferase in mouse tissues. Mol. Brain Res. 109, 146-160.

Huizing M. and Krasnewich D.M. (2009). Hereditary inclusion body myopathy: a decade of progress. Biochim. Biophys. Acta 1792, 881-887.

Krause S., Hinderlich S., Amsili S., Horstkorte R., Wiendl H., Argov Z., Mitrani-Rosenbaum S. and Lochmüller H. (2004). Localization of UDP-GlcNAc 2-epimerase/ManAc kinase (GNE) in the Golgi complex and the nucleus of mammalian cells. Exp. Cell Res. 304, 365-379.

Jay C., Nemunaitis G., Nemunaitis J., Senzer N., Hinderlich S., Darvish D., Ogden J., Eager J., Tong A. and Maples P.B. (2008). Preclinical Assessment of wt GNE Gene plasmid for management of Hereditary Inclusion Body Myopathy 2 (HIBM2). Gene Regul. and Syst. Biol. 2, 243-252.

Jay C.M., Levonyak N., Nemunaitis G., Maples P.B. and Nemunaitis J. (2009). Hereditary Inclusion Body Myopathy (HIBM2). Gene Regul. Syst. Biol. 3, 181-190.

Johnson D., Montpetit M.L., Stocker P.J. and Bennett E.S. (2004). The Sialic acid component of the β1 subunit modulates voltage-gated sodium channel function. J. Biol. Chem. 279, 44303-44310.

McDearmon E.L., Combs A.C. and Ervasti J.M. (2003). Core 1 glycans on α-dystroglycan mediate laminin-induced acetylcholine receptor clustering but not laminin binding. J. Biol. Chem. 278, 44868-44873.

Malicdan M.C., Noguchi S., Hayashi Y.K., Nonaka, I. and Nishino I. (2009). Prophylactic treatment with sialic acid metabolites preclude the development of a myopathic phenotype in the DMRV-hIBM mouse model. Nat. Med. 15, 690-695.

Malisan F., Franchi L., Tomassini B., Ventura N., Condò I., Rippo M.R., Rufini A., Liberati L., Nachtigall C., Kniep B. and Testi R. (2002). Acetylation suppresses the proapoptotic activity of GD3 ganglioside. J. Exp. Med. 196, 1535-1541.

Mandal C., Schwartz-Albiez R. and Vlasak R. (2015). Functions and biosynthesis of O-acetylated sialic acids. Top. Curr. Chem. 366, 1-30.

Marini M., Bonaccini L., Zappoli Thyrion G.D., Vichi D., Parretti E. and Sgambati E. (2011). Distribution of sugar residues in human placentas from pregnancies complicated by hypertensive disorders. Acta Histochem. 113, 815-825.

Marini M., Ambrosini S., Sarchielli E., Zappoli Thyrion G.D., Bonaccini L., Vannelli G.B. and Sgambati E. (2014). Expression of sialic acids in human adult skeletal muscle tissue. Acta histochem. 116, 926-935.

Mencucci R., Paladini I., Sarchielli E., Favuzza E., Vannelli G.B. and Marini M. (2013). Transepithelial riboflavin/ultraviolet. a corneal cross-linking in keratoconus: morphologic studies on human corneas. Am. J. Ophthalmol. 156, 874-884.

Mencucci R., Ambrosini S., Paladini I., Favuzza E., Boccalini C., Raugei G., Vannelli G.B. and Marini M. (2015). Early effects of corneal collagen cross-linking by iontophoresis in ex vivo human corneas. Graefes Arch. Clin. Exp. Ophthalmol. 253, 277-286.

Milman Krentsis I., Sela I., Eiges R., Blanchard V., Berger M., Becker Cohen M. and Mitrani-Rosenbaum S. (2011). GNE is involved in the early development of skeletal and cardiac muscle. PLoS One 6, e21389.

Murphy K.T., Ham D.J., Church J.E., Naim T., Trieu J., Williams D.A. and Lynch G.S. (2012). Parvalbumin gene transfer impairs skeletal muscle contractility in old mice. Hum. Gene Ther. 23, 824-836.

Nilsson J., Nilsson J., Larson G. and Grahn A. (2010). Characterization of site-specific O-glycan structures within the mucin-like domain of α-dystroglycan from human skeletal muscle. Glycobiology 20, 1160-1169.

North K.N., Wang C.H., Clarke N., Jungbluth H., Vainzo M., Dowling J.J., Amburgey K., Quijano-Roy S., Beggs A.H., Sewry C., Laing N.G. and Bönnemann C.G. (2014). Approach to the diagnosis of congenital myopathies. Neuromuscul. Disord. 24, 97-116.

O'Connell K., Gannon J., Doran P. and Ohlendieck K. (2008). Reduced expression of sarcalumenin and related Ca^{2+} -regulatory proteins in aged rat skeletal muscle. Exp. Gerontol. 43, 958-961.

Olguin H.C., Santander C. and Brandan E. (2003). Inhibition of myoblast migration via decorin expression is critical for normal skeletal muscle differentiation. Dev. Biol. 259, 209-224.

Olsen M., Zuber C., Roth J., Linnemann D. and Bock E. (1995). The ability to re-express polysialylated NCAM in soleus muscle after denervation is reduced in aged rats compared to young adult rats. Int. J. Dev. Neurosci. 13, 97-104.

Paccalet T., Coulombe Z. and Tremblay J.P. (2010). Ganglioside GM3 levels are altered in a mouse model of HIBM: GM3 as a cellular marker of the disease. PLoS One 5, e10055.

Rafuse V.F. and Landmesser L.T. (1996). The pattern of avian intramuscular nerve branching is determined by the innervating motoneuron and its level of polysialic acid. J. Neurosci. 20, 1056-1065.

Resende R.R., Andrade L.M., Oliveira A.G., Guimarães E.S., Guatimosim S. and Leite M.F. (2013). Nucleoplasmic calcium signaling and cell proliferation: calcium signaling in the nucleus. Cell Commun. Signal. 11, 14.

Rønn L.C., Berezin V. and Bock E. (2000). The neural cell adhesion molecule in synaptic plasticity and ageing. Int. J. Dev. Neurosci. 18, 193-199.

Saito F., Tomimitsu H., Arai K., Nakai S., Kanda T., Shimizu T., Mizusawa H. and Matsumura K.E. (2004). A Japanese patient with distal myopathy with rimmed vacuoles: missense mutations in the epimerase domain of the UDP-N-acetylglucosamine 2-epimerase/N-acetylmannosamine kinase (GNE) gene accompanied by hyposialylation of skeletal muscle glycoproteins. Neuromuscul. Disord. 14, 158-161.

Sanes J.R. (2003). The Basement membrane/basal lamina of skeletal muscle. J. Biol. Chem. 278, 12601-12604.

Schauer R. (2004). Sialic acids: fascinating sugar in higher animals and man. Zoology 107, 49-64.

Schauer R. (2009). Sialic acids as regulators of molecular and cellular interactions. Curr. Opin. Struct. Biol. 19, 507-514.

Schwetz T.A., Norring S.A., Ednie A.R. and Bennett E.S. (2011). Sialic acids attached to O-glycans modulate voltage-gated potassium channel gating. J. Biol. Chem. 286, 4123-4132.

Shibuya N., Goldstein I.J., Broekaert W.F., Nsimba-Lubaki M., Peeters B. and Peumans W.J. (1987). Fractionation of sialylated oligosaccharides, glycopeptides, and glycoproteins on immobilized elderberry (*Sambucus nigra* L.) barklectin. Arch. Biochem. Biophys. 254, 1-8.

Standring S. (2009). Anatomia del Grey. XL ed. Elsevier Masson.

Suzuki M., Angata K., Nakayama J. and Fukuda M. (2003). Polysialic acid and mucin type o-glycans on the neural cell adhesion molecule differentially regulate myoblast fusion. J. Biol. Chem. 278, 49459-49468.

Tajima Y., Uyama E., Go S., Sato C., Tao N., Kotani M., Hino H., Suzuki A., Sanai Y., Kitajima K. and Sakuraba H. (2005). Distalmyopathy with rimmed vacuoles: impaired O-glycan formationin muscular glycoproteins. Am. J. Pathol. 166, 1121-1130.

Varki A. (2007). Glycan-based interactions involving vertebrate sialic-acid-recognizing proteins. Nature 446 (7139), 1023-1029.

Varki A. and Schauer R. (2009). Sialic acids. In: Essentials of glycobiology. 2nd ed. Varki A., Cummings R.D., Esko J.D., Freeze H.H., Stanley P., Bertozzi C.R., Hart G.W. and Etzler M.E. (eds). Cold Spring Harbor Laboratory Press. New York. Chapter 14.

Voermans N.C., Guillard M., Doedée R., Lammens M., Huizing M., Padberg G.W., Wevers R.A., Van Engelen B.G. and Lefeber D.J. (2010). Clinical features, lectin staining, and a novel GNE frameshift mutation in HIBM. Clin. Neuropathol. 29, 71-77.

von Maltzahn J., Wulf V., Matern G. and Willecke K. (2011). Connexin39 deficient mice display accelerated myogenesis and regeneration of skeletal muscle. Exp. Cell Res. 317, 1169-1178.

Yi C.H., Vakifahmetoglu-Norberg H. and Yuan J. (2011). Integration of apoptosis and metabolism. Cold Spring Harb. Symp. Quant. Biol. 76, 375-387.

Yurchenco P.D. (2011). Basement membranes: Cell scaffoldings and signaling platforms. Cold Spring Harb. Perspect. Biol. 3, a004911.

Wang W.C., Clark G.F., Smith D.F. and Cummings R.D. (1988). Separation of oligosaccharides containing terminal alpha-linked galactose residues by affinity chromatography on *Griffonia simplicifolia* I bound to concanavalin A-sepharose. Anal. Biochem. 175, 390-396.

Zacharias N., Sailhamer E.A., Li Y., Liu B., Butt M.U., Shuja F., Velmahos G.C., de Moya M. and Alam H.B. (2011). Histone deacetylase inhibitors prevent apoptosis following lethal hemorrhagic shock in rodent kidney cells. Resuscitation 82, 105-109.

Accepted May 9, 2017